AIP | Review of Scientific Instruments

Method of mechanical holding of cantilever chip for tip-scan high-speed atomic force microscope

Shingo Fukuda, Takayuki Uchihashi, and Toshio Ando

Citation: Review of Scientific Instruments **86**, 063703 (2015); doi: 10.1063/1.4922381
View online: http://dx.doi.org/10.1063/1.4922381
View Table of Contents: http://scitation.aip.org/content/aip/journal/rsi/86/6?ver=pdfcov
Published by the AIP Publishing

REVIEW OF SCIENTIFIC INSTRUMENTS **86**, 063703 (2015)

Method of mechanical holding of cantilever chip for tip-scan high-speed atomic force microscope

Shingo Fukuda,[1] Takayuki Uchihashi,[1,2,3] and Toshio Ando[1,2,3]
[1]*Department of Physics, College of Science and Engineering, Kanazawa University, Kakuma-machi, Kanazawa 920-1192, Japan*
[2]*Bio-AFM Frontier Research Center, College of Science and Engineering, Kanazawa University, Kakuma-machi, Kanazawa 920-1192, Japan*
[3]*Core Research for Evolutional Science and Technology of the Japan Science and Technology Agency, 7 Goban-cho, Chiyoda-ku, Tokyo 102-0076, Japan*

(Received 23 February 2015; accepted 31 May 2015; published online 11 June 2015)

In tip-scan atomic force microscopy (AFM) that scans a cantilever chip in the three dimensions, the chip body is held on the Z-scanner with a holder. However, this holding is not easy for high-speed (HS) AFM because the holder that should have a small mass has to be able to clamp the cantilever chip firmly without deteriorating the Z-scanner's fast performance, and because repeated exchange of cantilever chips should not damage the Z-scanner. This is one of the reasons that tip-scan HS-AFM has not been established, despite its advantages over sample stage-scan HS-AFM. Here, we present a novel method of cantilever chip holding which meets all conditions required for tip-scan HS-AFM. The superior performance of this novel chip holding mechanism is demonstrated by imaging of the $\alpha_3\beta_3$ subcomplex of F_1-ATPase in dynamic action at ~7 frames/s. © *2015 AIP Publishing LLC.* [http://dx.doi.org/10.1063/1.4922381]

I. INTRODUCTION

High-speed atomic force microscopy (HS-AFM) was established around 2008[1] through long-range efforts to increase the response speed of cantilevers,[2,3] the scanner,[4–7] and electronics,[1,2,8] as well as to make the high-speed performance compatible with low-invasiveness to fragile samples[9] (see reviews[1,10,11]). This established HS-AFM has mainly been used to observe protein molecules in dynamic action at sub-100 ms to subsecond time resolution. For example, bacteriorhodopsin responding to light,[12] myosin V walking on actin filaments,[13] and rotor-less F_1-ATPase (i.e., the $\alpha_3\beta_3$ subcomplex of F_1-ATPase) with directional chemical-state rotation over the three β subunits[14] have been visualized (see reviews[15,16]). These observations have provided greater insights than ever before into how the proteins function, thus demonstrating the innovative power of this microscopy. Recently, fast wide-area scanners displaceable up to 23×23 μm^2 or up to ~50 $\times$ 50 μm^2 have been developed[17,18] together with a new vibration damping method for the wide-area scanners,[18] expanding the objects of HS-AFM observation to much larger ones. For example, various dynamic processes occurring in live bacterial and mammalian cells, such as endocytosis, membrane raffling, filopodia growth and bacteriolysis, were visualized within a few seconds.[18,19] The HS-AFM instrument used in these studies employs the sample stage-scan mode. To achieve the high scan rate and minimize the hydrodynamic effect of fast sample-stage movement on the cantilever behavior, a small sample stage (a glass rod with dimensions of 1–1.5 mm in diameter and 2 mm in height) is attached to the Z-scanner. This small size limits the range of specimens to be placed on the sample stage. Moreover, when the HS-AFM instrument is combined with an optical microscope, the optical image of the sample oscillates during HS-AFM imaging. More seriously, various optical microscopy techniques are incompatible with the configuration of mechanical and optical devices in the HS-AFM instrument, restricting the functional expansion of HS-AFM.

To overcome these limitations associated with the sample stage-scan mode, tip-scan HS-AFM has recently been attempted to be developed. One of the common requirements of tip-scan AFM that employs the widely used optical lever method of detecting cantilever's deflection is that the laser beam focused onto the cantilever should be able to track the lateral motion of the cantilever. This tracking adoptable to tip-scan HS-AFM was recently accomplished by laser beam scan in synchrony with the cantilever's lateral motion using either a mirror tilter[20] or a focusing lens embedded in the XY-scanner.[21] The combined system of total internal reflection fluorescence microscopy (TIRFM) and tip-scan HS-AFM equipped with the mirror tilter was demonstrated to be able to capture topographic AFM and single-molecule fluorescent images simultaneously at a few frames/s (fps).[20] Thus, tip-scan HS-AFM opened new opportunities to observe dynamic events in a large specimen placed on the stage of an inverted optical microscope as well as to combine HS-AFM with various optical techniques, such as super-resolution fluorescence microscopy techniques[22,23] and even optical tweezers.[24]

Nevertheless, an important issue, which is seemingly simple but practically difficult to resolve, has remained to be accomplished. That is, how to attach a cantilever chip firmly onto the fast, lightweight Z-scanner, without deteriorating the fast, precise response of the Z-scanner. As a matter of course, one can firmly glue a cantilever chip onto the Z-scanner, as has been done in the above tip-scan HS-AFM/TIRFM experiments. However, the chip has to be frequently replaced with a new one, and therefore, this method is inadequate for routine use. The use of thermoplastic adhesives is one possibility.

However, the adhesives cannot be removed completely but partially remain after removal of the cantilever and gradually age by repeated heating, resulting in a rough surface of the Z-scanner's top face. Moreover, when the cantilever is immersed in a buffer solution, such adhesives contaminate the solution. The conditions required for the method of holding a cantilever chip are as follows: (i) a cantilever chip body has to be firmly clamped so that the chip does not generate unwanted vibrations during fast scanning of the Z-scanner, (ii) the cantilever chip holder has to have a small mass and the first resonant frequency higher than that of the Z-scanner, (iii) a cantilever chip has to be easily attached onto and removed from the Z-scanner so that the scanner would not be damaged during these operations, and (iv) the cantilever chip holder should be durable without aging and wear so as to be used repeatedly.

Magnetic or vacuum clamp may be a possible candidate but magnetic clamp requires ferromagnetic coating of a cantilever chip, which is inadequate for routine use, while vacuum clamp is too weak to hold a cantilever chip firmly enough not to generate unwanted vibrations. Therefore, mechanical clamp seems to be a only candidate that would meet all the required conditions. However, the entire body of the mechanical clamping system cannot be mounted directly on the Z-scanner. This is partly because the mass effect of this mounting would significantly reduce the resonant frequency of the Z-scanner and primarily because repeated exchange of cantilever chips would damage the Z-scanner (e.g., the Z-piezoactuator is unglued from the supporting base). In fact, this way of mounting was recently shown by Fukuma's group to deteriorate the frequency response of the Z-scanner even in the best case among various designs.[25] Our group also has experienced this problem as well as the damaging problem. Therefore, we here tested methods in which a cantilever chip clamping system was indirectly mounted on the Z-scanner and reached a design that did not affect the fast, precise response of the Z-scanner. This excellent performance was demonstrated by imaging of protein molecules in dynamic action.

II. EXPERIMENTAL SETUP

The scanner used here is similar to that developed previously for tip-scan HS-AFM,[20] except its modification for cantilever chip holding. Briefly, for the Z-scanner, the stack piezoactuator (AE0203D04F Tokin-NEC, Miyagi, Japan) is used that has dimensions $2 \times 3 \times 5$ mm^3, the measured first resonant frequency in free oscillation 222 kHz (nominally 261 kHz), and the measured displacement efficiency 18.2 nm/V (nominal maximum displacement, 4.6 μm at 150 V). This Z-piezoactuator is glued onto the top of the supporting base to be scanned in the X- and Y-directions. The same type of a piezoactuator (Z′-piezoactuator) is also glued onto the bottom of the supporting base to counteract the impulsive force produced by quick displacement of the Z-piezoactuator.[3] The gap space in the scanner is filled with an elastomer having a high loss factor to absorb the mechanical vibration energy.[18] A wedge-shaped stage (hereafter referred to as "w-stage") on which a cantilever chip to be placed is glued onto the top of the Z-scanner. This w-stage (32 mg) is made of silicon carbide with a high Young's modulus-to-density ratio (Young's

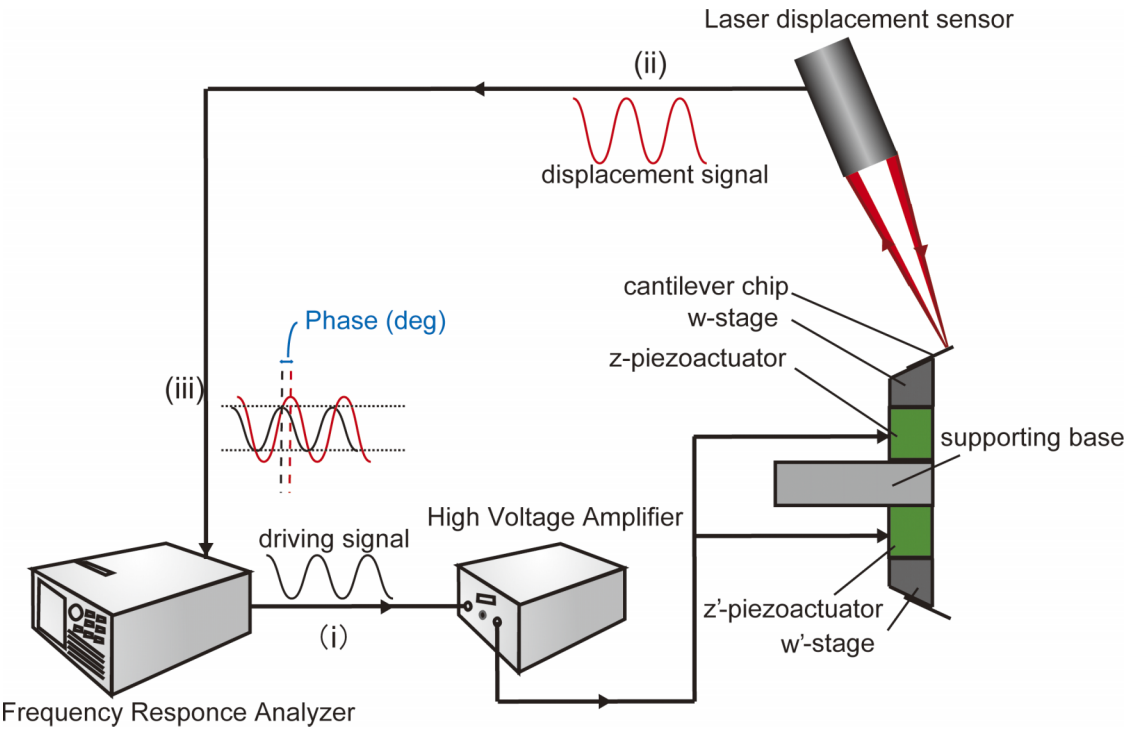

FIG. 1. Experimental setup for the characterization of Z-scanner's frequency response. (i) Frequency response analyzer (FRA) simultaneously drives the Z- and Z′-piezoactuators with sinusoidal waves at various frequencies through a high-bandwidth piezodriver. (ii) The laser displacement sensor detects the displacement of target portions (i.e., the top face of the Z-scanner without both w-stage and cantilever chip holder, the top face of the w-stage, and the distal portion of the cantilever chip body). (iii) The FRA calculates the gain and phase of the signal from the sensor. The phase is relative to the driving signal.

modulus, ~430 GPa; density, ~3.2 g/cm^3). The wedge angle is 20°, so that the mounted cantilever is tilted by this angle with respect to the sample substrate. To facilitate guiding of a cantilever chip onto the w-stage, a shallow groove slightly wider than the cantilever chip is cut on the top face of the w-stage. Another wedge-shaped stage (w′-stage) identical to the w-stage is also glued on the top of the Z′-piezoactuator as counterweight.

The experimental setup for analyzing the frequency responses described below is illustrated in Fig. 1. For the frequency response analysis, a frequency response analyzer (FRA5097, NF Corp., Kanagawa, Japan) was used. For the analysis of the frequency response of the Z-scanner itself, the w- and w′-stages were removed from the Z- and Z′-piezoactuators, respectively. The Z- and Z′-piezoactuators were simultaneously and sinusoidally oscillated in synchrony with each other at amplitude of 6 nm and frequencies of 0–400 kHz through a high-bandwidth (~1 MHz) piezodriver (M-2335, custom-made, Mess-Tek. Corp., Saitama, Japan). A heterodyne laser displacement sensor (ST-3761, IWATSU, Tokyo, Japan) was used to measure mechanical vibrations occurring at target portions. Its laser beam was incident on the Z-scanner without the w- and w′-stages, the w-stage glued onto the Z-scanner (the w′-wage was also glued to the Z′-piezoactuator) or the cantilever chip (BL-AC7DS-KU5, custom-made, Olympus, Tokyo, Japan) clamped on the w-stage with either of the two cantilever chip holding mechanisms described below (note that an identical cantilever chip was glued to the w′-stage as counterweight). For the measurement of cantilever chip vibrations, the laser was incident on the cantilever chip body at a distal position from which the cantilever extends. Note that for the vibration measurements, we could not use the optical beam deflection sensor equipped in our tip-scan HS-AFM instrument because this sensor detects an angle change of the target rather than its displacement. The solid lines in Fig. 2 show the frequency response of the Z-scanner itself, indicating the first resonant frequency of the one-end-fixed Z-piezoactuator, 110 kHz, as expected from the measured resonant frequency of the piezoactuator in free oscillation, 222 kHz. The attachment of the w-stage on the top of the Z-scanner only slightly changed the frequency response of the Z-scanner, as shown with the dotted lines in Fig. 2.

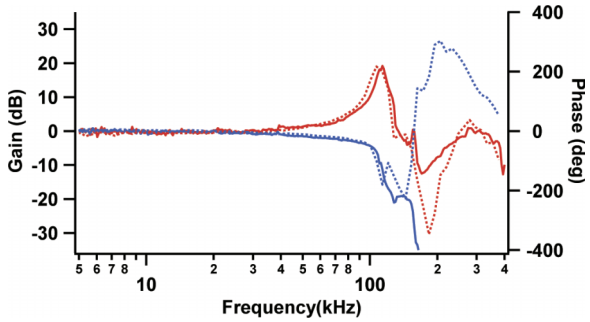

FIG. 2. Frequency responses of one-end-fixed Z-piezoactuator with and without w-stage. The solid lines (red line, gain; blue line, phase) indicate the frequency response in the case without w-stage, while the dotted lines (red line, gain; blue line, phase) indicate the frequency response in the case with the w-stage.

III. CANTILEVER CHIP HOLDING MECHANISMS

To avoid damaging the Z-scanner by repeated exchange of cantilever chips, the entire chip holder should not be directly mounted on the top of the Z-scanner. Otherwise, a pushing force (or torque) exerted by an operator to the chip holder is directly applied onto the Z-scanner, often resulting in damage of the Z-scanner or ungluing of the holder from the Z-scanner. The entire mounting is also inadequate in another regard; it would result in that we have to clamp a cantilever chip firmly with a small-sized lightweight mechanism. But, it is difficult. When the holding mechanism is relatively heavy, it significantly impairs the Z-scanner's resonant frequency; a Z-piezoactuator to be used for HS-AFM is small and its mass is approximately in the range of 100–300 mg. As such, the chip holder should be supported on one prop or two props standing on the base block onto which the Z-piezoactuator is glued. Moreover, the holder should have a simple structure so as to achieve high resonant frequencies.

Considering these factors, we first designed a holding mechanism in which the clamping system is supported on a single prop, as shown in Fig. 3. The prop was monolithically fabricated on the base block mentioned above (stainless steel SUS303). The prop is positioned at the back of the Z-piezoactuator. The top face of the prop is slanted from the horizontal plane at an angle the same as the wedge angle of

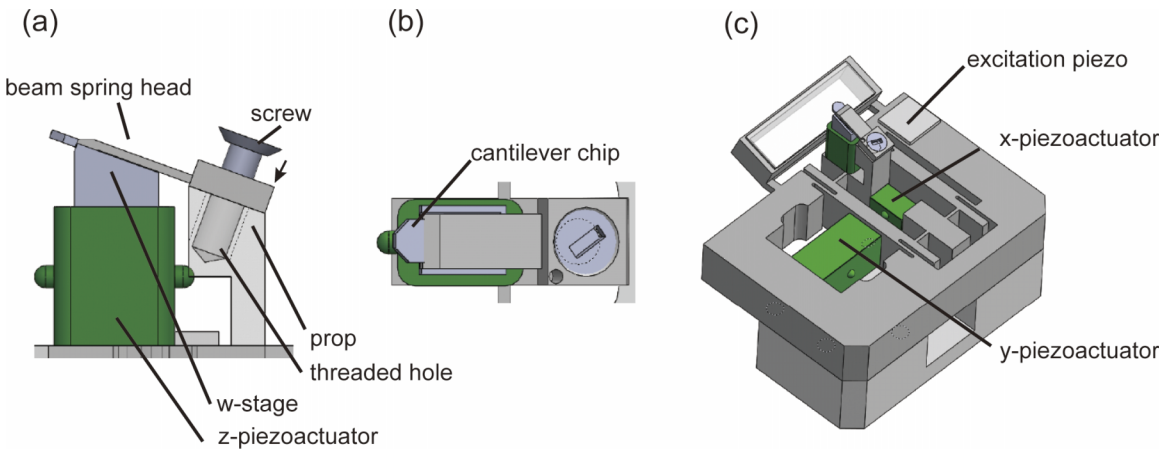

FIG. 3. Schematic diagram of the scanner with single-prop holding mechanism. (a) Side view, (b) top view, and (c) whole view.

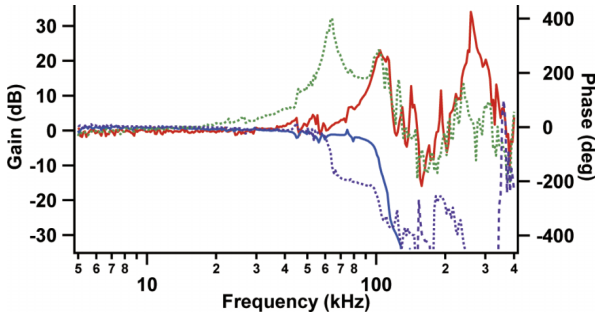

FIG. 4. Frequency responses of Z-scanner equipped with single-prop holding mechanism with and without elastic polymer sheet on the beam spring head. The solid lines (red line, gain; blue line, phase) indicate the frequency response in the case with the polymer sheet. The dotted lines (green, gain; purple, phase) indicate the frequency response in the case without the polymer sheet.

the w-stage, 20°. The top part of the prop is internally threaded perpendicularly to the slanted plane. One end of a beam spring (stainless steel SUS303) with the total length of 7.15 mm is clamped on the slanted top face of the prop with a screw so that the cantilever inserted between the beam spring head and the w-stage is pushed down onto the w-stage. Note that the height of the prop is adjusted so that clamping force can be applied from the beam spring to the cantilever chip. That is, the top face of the prop is positioned lower by 0.1 mm than the top surface of the installed cantilever chip body. To keep the beam spring head from touching the sample of observation, its distal edge region is cut aslant at an angle of 20°. The dotted lines in Fig. 4 indicate the frequency response of the cantilever chip held by this method, indicating appearance of an extra resonant peak at ~63 kHz, which is followed by a resonant peak at 105 kHz that originates from the w-stage-mounted Z-scanner itself (compare the spectra to those shown with the dotted lines in Fig. 2). The extra resonant vibrations at ~63 kHz indicate that the cantilever chip vibrates at the resonant frequency of the beam spring that insufficiently clamps the chip. This insufficiency may result from incomplete contact between the surface of the beam spring head (0.8×1.9 mm^2) and the cantilever chip body, which is very likely to be due to the deformation of the beam spring by clamping. To test this possibility and increase the contact area, an elastic polymer sheet was attached on the bottom surface of the beam spring head at its area to be in contact with the cantilever chip. This sheet (thickness ~50 μm) was prepared by thin coating of the beam spring head with an adhesive (Super-X, Cemedine, Tokyo, Japan) and then drying. As shown with the solid red lines in Fig. 4, the large resonant peak at ~63 kHz disappeared by this treatment, suggesting a larger clamp force as well as an additional role of the polymer sheet as a vibration damper; however, small resonant peaks around 50 kHz remained.

To increase the clamping force, we then designed another chip holding mechanism in which a beam spring was bridged between and supported by two props standing by the Z-piezoactuator, as shown in Fig. 5. As done for the single-prop system, the height of the props is adjusted, the top face of each prop is slanted from the horizontal plane at an angle of 20°, and the top part of each prop is internally threaded perpendicularly to the slanted plane. The each end of a beam spring (stainless steel SUS303) that is 9.6 mm long, 3.5 mm wide, and 0.3 mm thick was clamped on the corresponding prop using a screw to push the inserted cantilever chip onto the w-stage. The distal edge region (width, 0.97 mm) of the beam spring is cut aslant at an angle of 20° (see Figs. 5(b) and 5(c). As shown with the dotted lines in Fig. 6(a), even without elastic polymer coating of the beam spring, the frequency response of a cantilever chip held in this method was similar to that of the w-stage-mounted Z-piezoactuator itself (see the green line in Fig. 6(b) showing the difference amplitude spectrum between those measured at the w-stage without the clamp system and at the clamped cantilever chip body), suggesting less deformation of the beam spring than the case of the single-prop system. When the beam spring was coated with an elastic polymer film as above, the frequency response was improved, as shown with the solid lines in Fig. 6(a), while the main resonant frequency was only slightly lowered from 108 kHz to 102 kHz. This vibration damping effect of the polymer coating is more clearly shown with the red line in Fig. 6(b) that indicates the difference amplitude spectrum between those measured at the w-stage without the clamp system and at the cantilever chip body that is clamped with the polymer-coated beam spring. Note that pushing forces exerted from an operator are not directly applied to the cantilever chip (and hence to the Z-scanner) but partially and indirectly exerted from the

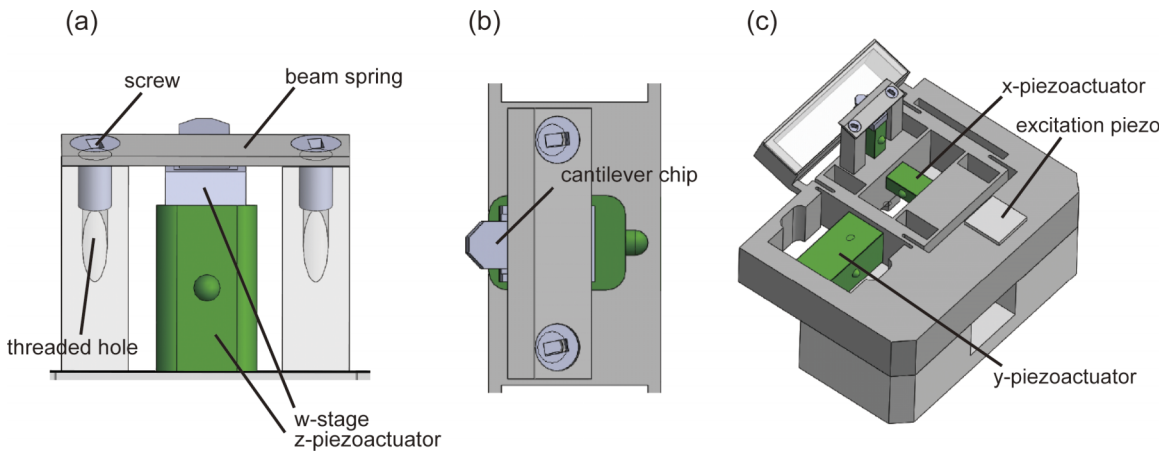

FIG. 5. Schematic diagram of the scanner with two-prop holding mechanism. (a) Side view, (b) top view, and (c) whole view.

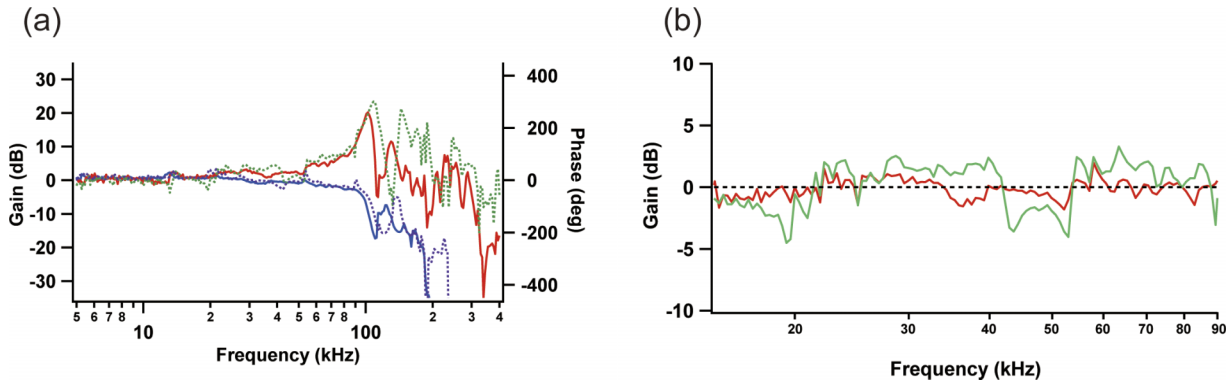

FIG. 6. Frequency responses of Z-scanner equipped with two-prop holding mechanism with and without elastic polymer sheet on the beam spring. (a) The solid lines (red line, gain; blue line, phase) indicate the frequency response in the case with the polymer sheet. The dotted lines (green, gain; purple, phase) indicate the frequency response in the case without the polymer sheet. These responses were measured at the cantilever chip body held in this mechanism. (b) Differential amplitude spectra between two cases: one is measured at the mounted cantilever chip body, whose data are the same as those shown in (a), and another is measured at the w-stage without the cantilever holing mechanism, which is shown with the red dotted line in Fig. 2 (the former was subtracted from the latter). The green and red lines indicate the cases without and with an elastic polymer sheet on the beam spring, respectively.

beam spring. Moreover, the magnitude of the force applied from the beam spring to the cantilever chip is restricted by the spring constant of the beam spring (~400 N/mm) as well as by the height difference (0.1 mm) between the top surfaces of the props and the top surface of the mounted cantilever chip. The upper limit of the force is further reduced by the polymer film coated on the beam spring. The cantilever chip can be easily removed from the holder by loosening of the screws. As such, the Z-scanner would not be damaged by repeated exchange of cantilever chips. Moreover, the displacement efficiency of the Z-scanner with a cantilever chip held in this method was 15.2 nm/V, similar to that of the Z-scanner alone (18.2 nm/V). This slight reduction is consistent with the loaded force (~30 N) and the maximum force that can be generated by the piezoactuator (~200 N).

However, a minor drawback was that the base block to be moved by the X- and Y-scanners became heavier because the base block was needed to be larger to accommodate the

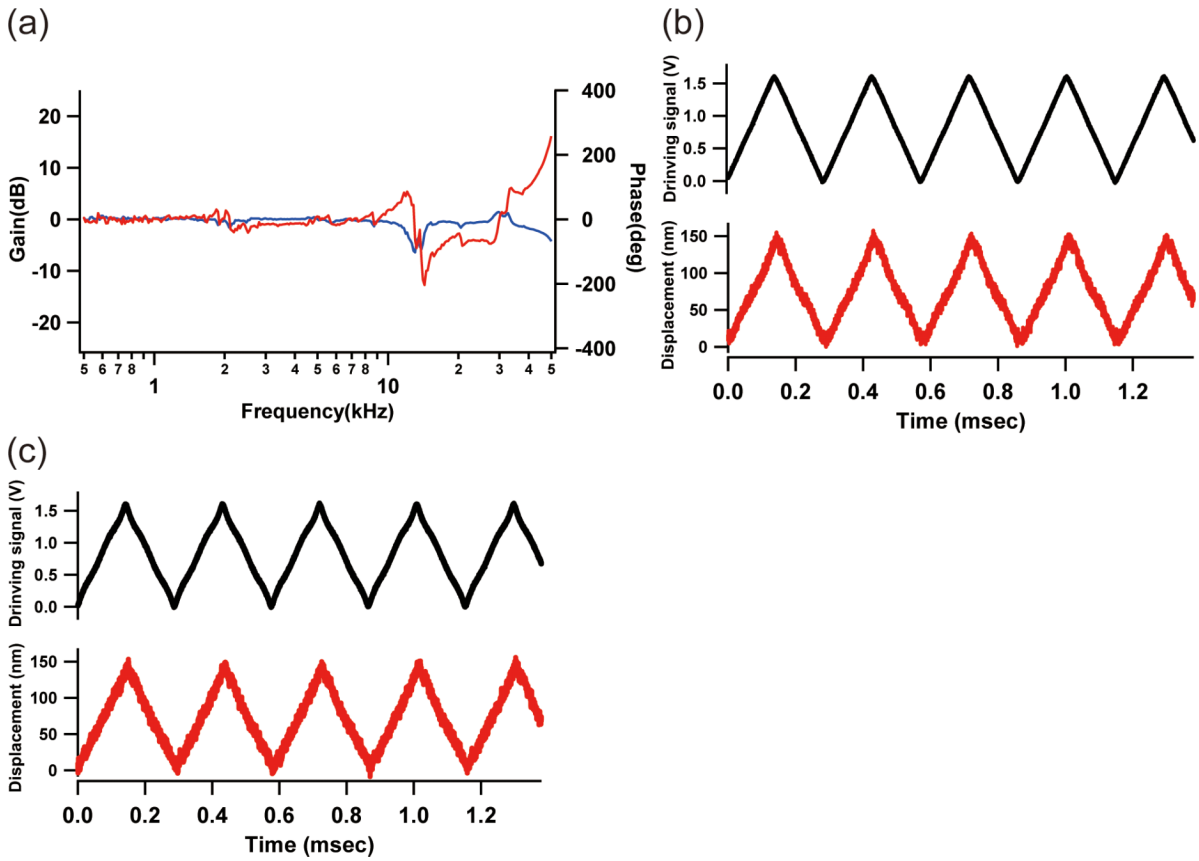

FIG. 7. Effect of inverse feedforward compensation on the displacement of the X-scanner. (a) Frequency response of the X-scanner (red line, gain; blue line, phase). (b) X-scanner displacement (red line) when driven by 3.45 kHz isosceles triangle wave signal (black line). (c) X-scanner displacement (red line) when driven by 3.45 kHz isosceles triangle signal filtered through inverse compensation (black line).

two props thereon, and therefore, the resonant frequency of the X-scanner was lowered from 18 kHz to 10 kHz, while the resonant frequency of the Y-scanner was lowered from 1.5 kHz to 1.3 kHz (the frequency response of the X-scanner is shown in Fig. 7(a)). Nonetheless, the lowered resonant frequency of the X-scanner is within a range that the adverse responses of the X-scanner can be removed by using an inverse feedforward compensation method as described previously.[18,26] In fact, this removal of adverse responses was proven, as follows. When the X-scanner was driven with triangle signals of 3.45 kHz (black line in Fig. 7(b)), its displacement exhibited small vibrations (see slightly waved displacements shown with the red line in Fig. 7(b)). However, it was displaced smoothly (red line in Fig. 7(c)) when driven with 3.45 kHz triangle wave signals that were modified by the inverse feedforward compensation method (black line in Fig. 7(c)). The filter used in this signal modification was constructed using the frequency response spectra of the X-scanner (Fig. 7(a)). When 100 scan lines are used, this scan frequency corresponds to the imaging rates of ~34 fps. The Y-scanner is usually driven by a saw-tooth wave containing a precipitous downward regime where the tip is returned to the scan origin. When the Y-scanner is scanned fast, it generates significant vibrations in this regime, which then decay while ringing in the following slow upward regime. This vibration generation can be easily be suppressed by the scan speed being lowered only in the precipitous downward regime, as described previously.[17] The time delay added by this slower scan is negligible because it is much shorter than the frame imaging time.

IV. IMAGING OF PROTEIN MOLECULES

Here, we demonstrate the superior performance of the cantilever chip holding method developed above (two-prop type) by imaging the $\alpha_3\beta_3$ subcomplex of F_1-ATPase in the presence of 2 μM adenosine triphosphate (ATP), using our tip-scan HS-AFM setup developed previously.[20] The imaging was carried out in amplitude modulation mode, with cantilever oscillation amplitude of ~2 nm. The cantilever used was BL-AC7DS-KU5 (Olympus, Tokyo, Japan) with resonant frequencies of 3.5 MHz in air and 1.2 MHz in water and a spring constant of ~0.2 N/m. The protein sample and the assay system for HS-AFM observation were prepared as described previously.[14] Figure 8 shows successive AFM images captured at 7.14 fps, which display conformational dynamics occurring in the $\alpha_3\beta_3$ subcomplex during ATP hydrolysis. It is visible in the images that the three β subunits undergo a conformational transition between the high (i.e., nucleotide-free) and low (i.e., nucleotide-bound) states. In Fig. 8, a highest pixel position in each frame is marked with a red closed circle. Therefore, it can be seen that the position of the nucleotide-free β subunit shifts counterclockwise. The rate constant of this shift was comparable to the value obtained previously from images of the $\alpha_3\beta_3$ subcomplex captured by sample stage-scan HS-AFM at 12.5 fps.[14] We attempted to image at the same rate using the tip-scan HS-AFM system but could not do so. This is solely because the resonant frequency of the one-end-fixed Z-piezoactuator used in the tip-scan HS-AFM apparatus (i.e., 110 kHz) is lower than that of the one-end-fixed Z-piezoactuator (PL033.30, Physik Instrumente (PI) GmbH, Karlsruhe, Germany) used in the sample stage-scan HS-AFM apparatus (~180 kHz).

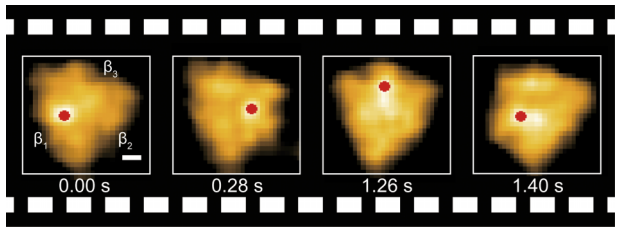

FIG. 8. Successive AFM images of the $\alpha_3\beta_3$ subcomplex of F_1-ATPase showing counterclockwise propagation of conformational changes over the three β subunits. Frame rate, 7.14 fps; scale bar, 2 nm. The highest pixel position in each frame image is marked with a closed red circle.

V. CONCLUSION

In this study, we solved one of the difficult issues in establishing tip-scan HS-AFM, i.e., how to hold a cantilever chip on the Z-scanner. The holding mechanism developed in this study only slightly lowered the resonant frequency and displacement efficiency of the Z-piezoactuator (<10% and ~16%, respectively) and lowered the resonant frequencies of the X- and Y-scanners by ~44% and ~13%, respectively. The relatively large reduction of the X-scanner's resonant frequency is due mainly to the increased size (by ~400%) of the base block to be displaced by the X-scanner. However, the resulted resonant frequency of the X-scanner (10 kHz) is not the main factor that limits the imaging rate, as demonstrated above using the inverse feedforward compensation method. Even for the wide-area scanner displaceable up to $\sim 50 \times 50$ μm^2 in the X- and Y-directions, this compensation method permits its X-scanner with the first resonant frequency of ~2 kHz to be displaced at 1 kHz approximately in an isosceles triangle form as a function of time, without producing unwanted vibrations.[18] Rather, the Z-scanner's resonant frequency severely limits the imaging rate because the feedforward compensation technique cannot be applied to the Z-scanner.

By the combination of the chip holding mechanism developed here together with the mirror tilter system for laser beam tracking of the lateral motion of the cantilever, tip-scan HS-AFM is now established. Note that other devices for HS-AFM have already been established in the course of the development of sample stage-scan HS-AFM. By this establishment of tip-scan HS-AFM, we can now apply large and/or heavy specimens to HS-AFM imaging, such as live cells in a culture dish and a semiconductor wafer. Moreover, various optical techniques can be combined with tip-scan HS-AFM, such as optical tweezers and super-resolution and tip-enhanced[27,28] fluorescence microscopy techniques. This large expansion of the applicable samples and the functionality will significantly increase the usefulness of tip-scan HS-AFM not only in life science but also in industrial inspection, testing, and measurements.

However, for the use of tip-scan HS-AFM in liquid environment, one minor issue remaining to be resolved is to make the Z-piezoactuator waterproof because it has to be located

closer to the cantilever chip covered with a liquid than in the case of sample stage-scan HS-AFM. This is the reason that we used the waterproof piezoactuator AE0203D04F (Tokin-NEC, Miyagi, Japan) despite its lower resonant frequency than the non-waterproof piezoactuator PL033.30 (PI GmbH, Karlsruhe, Germany).

ACKNOWLEDGMENTS

We thank Dr. R. Iino for providing us with the sample of puried $\alpha_3\beta_3$ subcomplex. This work was supported by the CREST program of the Japan Science and Technology Agency (JST) (to T.A.), the JST program on Development of Systems and Technology for Advanced Measurement and Analysis (to T.A.), KAKENHI for Basic Research (No. 24227005 to T.A. and Nos. 23115008, 24241048, 26104514, and 26102515 to T.U.), and KAKENHI for Scientific Research on Innovative Areas: Research in a Proposed Research Area (No. 26119003 to T.A.) and Grant-in-Aid for Research Fellows (to S.F.) from the Japan Society for the Promotion of Science.

[1]T. Ando, T. Uchihashi, and T. Fukuda, Prog. Surf. Sci. **83**, 337 (2008).
[2]T. E. Schäffer, J. P. Cleveland, F. Ohnesorge, D. A. Walters, and P. K. Hansma, J. Appl. Phys. **80**, 3622 (1996).
[3]T. Ando, N. Kodera, E. Takai, D. Maruyama, K. Saito, and A. Toda, Proc. Natl. Acad. Sci. U. S. A. **98**, 12468 (2001).
[4]G. E. Fantner, G. Schitter, J. H. Kindt, T. Ivanov, K. Ivanova, R. Patel, N. Holten-Andersen, J. Adams, P. J. Thuner, I. W. Rangelow, and P. K. Hansma, Ultramicroscopy **106**, 881 (2006).
[5]T. Ando, T. Uchihashi, N. Kodera, A. Miyagi, R. Nakakita, H. Yamashita, and K. Matada, e-J. Surf. Sci. Nanotechnol. **3**, 384 (2005).
[6]N. Kodera, H. Yamashita, and T. Ando, Rev. Sci. Instrum. **76**, 053708 (2005).
[7]T. Fukuma, Y. Okazaki, N. Kodera, T. Uchihashi, and T. Ando, Appl. Phys. Lett. **92**, 243119 (2008).
[8]G. E. Fantner, P. Hegarty, J. H. Kindt, G. Schitter, G. A. G. Cidade, and P. K. Hansma, Rev. Sci. Insturm. **76**, 026118 (2005).
[9]N. Kodera, M. Sakashita, and T. Ando, Rev. Sci. Instrum. **77**, 083704 (2006).
[10]Y. K. Yong, S. O. R. Moheimani, B. J. Kenton, and K. K. Leang, Rev. Sci. Instrum. **83**, 121101 (2012).
[11]T. Ando, Nanotechnology **23**, 062001 (2012).
[12]M. Shibata, H. Yamashita, T. Uchihashi, H. Kandori, and T. Ando, Nat. Nanotechnol. **5**, 208 (2010).
[13]N. Kodera, D. Yamamoto, R. Ishikawa, and T. Ando, Nature **468**, 72 (2010).
[14]T. Uchihashi, R. Iino, T. Ando, and H. Noji, Science **333**, 755 (2011).
[15]T. Ando, T. Uchihashi, and N. Kodera, Annu. Rev. Biophys. **42**, 393 (2013).
[16]T. Ando, T. Uchihashi, and S. Scheuring, Chem. Rev. **114**, 3120 (2014).
[17]C. Braunsmann and T. E. Schäffer, Nanotechnology **21**, 225705 (2010).
[18]H. Watanabe, T. Uchihashi, T. Kobashi, M. Shibata, J. Nishiyama, R. Yasuda, and T. Ando, Rev. Sci. Instrum. **84**, 053702 (2013).
[19]M. Shibata, T. Uchihashi, T. Ando, and R. Yasuda, Sci. Rep. **5**, 8724 (2015).
[20]S. Fukuda, T. Uchihashi, R. Iino, Y. Okazaki, M. Yoshida, K. Igarashi, and T. Ando, Rev. Sci. Instrum. **84**, 073706 (2013).
[21]Y. Suzuki, N. Saskai, A. Yoshida, Y. Uekusa, A. Yagi, Y. Imaoka, S. Ito, K. Karaki, and K. Takeyasu, Sci. Rep. **3**, 2131 (2013).
[22]L. Schermelleh, R. Heintzmann, and H. Leonhardt, J. Cell Biol. **190**, 165 (2010).
[23]B. Harke, J. V. Chacko, H. Haschke, C. Canale, and A. Diaspro, Opt. Nanosc. **1**, 3 (2012).
[24]K. C. Neuman and S. M. Brock, Rev. Sci. Instrum. **75**, 2787 (2004).
[25]S. M. R. Akrami, K. Miyata, H. Asakawa, and T. Fukuma, Rev. Sci. Instrum. **85**, 126106 (2014).
[26]G. Schitter and A. Stemmer, IEEE Trans. Control Syst. Technol. **12**, 449 (2004).
[27]Z. Ma, J. M. Gerton, L. A. Wade, and S. R. Quake, Phys. Rev. Lett. **97**, 260801 (2006).
[28]O. J. F. Martin and C. Girard, Appl. Phys. Lett. **70**, 705 (1997).